Evaluation of Level-Crossing ADCs for Event-Driven ECG Classification

Maryam Saeed, Qingyuan Wang, Olev Martens, Benoit Larras, Antoine Frappé, Barry Cardiff, John Deepu

This article has been accepted for publication in a future issue of this journal, but has not been fully edited. Content may change prior to final publication. Citation information: DOI 10.1109/TBCAS.2021.3136206, IEEE Transactions on Biomedical Circuits and Systems

Evaluation of Level-Crossing ADCs for Event-Driven ECG Classification

Maryam Saeed, *Graduate Student Member, IEEE*, Qingyuan Wang, *Graduate Student Member, IEEE*, Olev Märtens, *Senior Member, IEEE*, Benoit Larras, Antoine Frappé, *Senior Member, IEEE*, Barry Cardiff, *Senior Member, IEEE*, Deepu John, *Senior Member, IEEE*

***Abstract*—In this paper, a new methodology for choosing design parameters of level-crossing analog-to-digital converters (LC-ADCs) is presented that improves sampling accuracy and reduces the data stream rate. Using the MIT-BIH Arrhythmia dataset, several LC-ADC models are designed, simulated and then evaluated in terms of compression and signal-to-distortion ratio. A new one-dimensional convolutional neural network (1D-CNN) based classifier is presented. The 1D-CNN is used to evaluate the event-driven data from several LC-ADC models. With uniformly sampled data, the 1D-CNN has 99.49%, 92.4% and 94.78% overall accuracy, sensitivity and specificity, respectively. In comparison, a 7-bit LC-ADC with 2385Hz clock frequency and 6-bit clock resolution offers 99.2%, 89.98% and 91.64% overall accuracy, sensitivity and specificity, respectively. It also offers 3x data compression while maintaining a signal-to-distortion ratio of 21.19dB. Furthermore, it only requires 49% floating-point operations per second (FLOPS) for cardiac arrhythmia classification in comparison with the uniformly sampled ADC. Finally, an open-source event-driven arrhythmia database is presented.**

***Index Terms*—level-crossing ADC, cardiac arrhythmia classification, convolutional neural networks, wearable sensors, event-driven data**

I. Introduction

In recent years, the number of portable wireless biomedical systems have grown exponentially facilitating better health care monitoring and earlier diagnosis [1]. As a result, high volumes of data are produced with increasing number of biomedical sensors and long-term monitoring. In these biomedical signal monitoring systems, the energy consumption of wireless communication modules generally exceeds all other modules combined, for example in [2], [3], it is reported that the wireless module consumes up-to two-thirds of the total power on-chip. To reduce energy consumption, on-chip feature extraction and compression techniques are applied after sampling from an analog-to-digital converter (ADC) [4]–[8]. Recently, a new class of ADCs, called level-crossing ADCs (LC-ADCs), has been developed which embed compression into the data acquisition stage [9]–[12]. LC-ADCs utilize the time-domain sparsity of signals, such as, electrocardiogram (ECG) signals, which remain inactive for large time intervals. LC-ADCs produce asynchronous samples of data triggered by the threshold crossings of the analog signal. This reduces the sampling in low-activity regions of the signal, thus reducing the data rate and energy consumption on-chip. LC-ADCs have the advantage of built-in compression and a corresponding potential reduction in processing costs in comparison with Nyquist sampling ADCs.

The energy efficiency of a LC-ADC and traditional successive-approximation (SAR) ADC using various biosignals was studied in [9]. They concluded that LC-ADCs are more energy-efficient than SAR ADCs for low-to-medium resolution applications, while also producing less data for transmission.Many low-power LC-ADC architectures have been proposed in recent years for various biomedical applications, such as biomedical signal acquisition [3], [13]–[16], ultrasound measurement systems [17], ECG signal acquisition [10], low-power QRS detection in ECG signals [11], [18], low data rate image sensors [19], and a reconfigurable event-driven wake-up system [20]. Moreover, classification algorithms have been widely designed for various biomedical applications using traditional SAR ADCs. A detailed review of classification algorithms, their hardware designs and power consumption is presented in [21]. Recently, ECG signals have also been used for low-power authentication of devices which also utilizes neural networks and compression techniques [22]. Using event-driven data from LC-ADCs, an artificial neural network based arrhythmia classification has been presented in [12].

This article builds on the work presented in [23], which evaluated several level-crossing ADC models for cardiac arrhythmia classification and compression performance. To the best of our knowledge, no other performance analysis of LC-ADC models for event-driven ECG classification is found in the literature. In this article, we propose a new design strategy for modeling LC-ADC parameters inspired by the work presented in [3] and apply it to low-power event-driven cardiac arrhythmia classification. In this context, the major contributions of this paper are as follows: a) a new design technique for modeling level-crossing ADC parameters is presented that improves sampling accuracy and reduces data stream rate from the LC-ADC, b) several LC-ADC models

This work is supported by 1) JEDAI project under the Chist-Era Program; 2) Schlumberger Foundation's Faculty for the Future Program 3) Microelectronic Circuits Centre Ireland and 4) Science Foundation Ireland through the SFI Centre for Research Training in Machine Learning (18/CRT/6183). *Corresponding author: Deepu John*

M. Saeed, Q. Wang, B. Cardiff, and D. John are with the School of Electrical and Electronic Engineering, University College Dublin, Ireland. Email:{maryam.saeed, qingyuan.wang}@ucdconnect.ie, {barry.cardiff, deepu.john}@ucd.ie

O. Märtens is with the Tallinn University of Technology, Estonia. Email: olev.martens@taltech.ee

B. Larras and A. Frappé are with the Univ. Lille, CNRS, Centrale Lille, Junia, Univ. Polytechnique Hauts-de-France, UMR 8520-IEMN, France. Email:{benoit.larras, antoine.frappe}@junia.com,

This article has been accepted for publication in a future issue of this journal, but has not been fully edited. Content may change prior to final publication. Citation information: DOI 10.1109/TBCAS.2021.3136206, IEEE Transactions on Biomedical Circuits and Systems

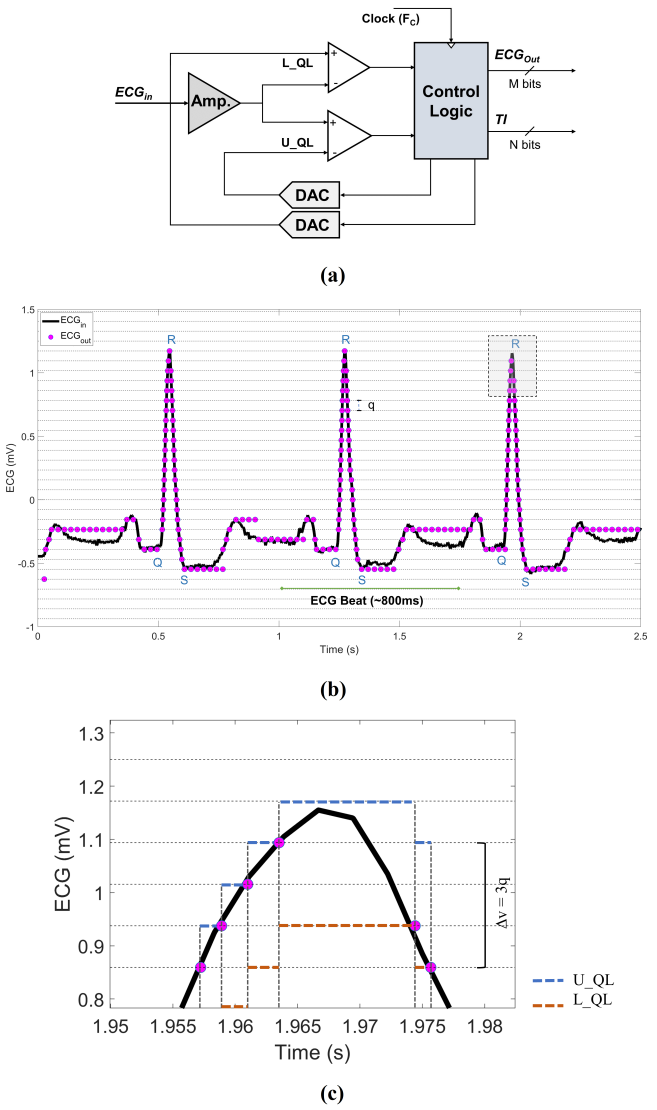

Fig. 1: (a) a level-crossing ADC architecture (b) event-driven ECG samples (ECG_{out}), the analog ECG signal (ECG_{in}), and horizontal lines indicating the quantization levels using a 7-bit LC-ADC. (c) illustrated threshold crossings with LSB size, Δv = 3q.

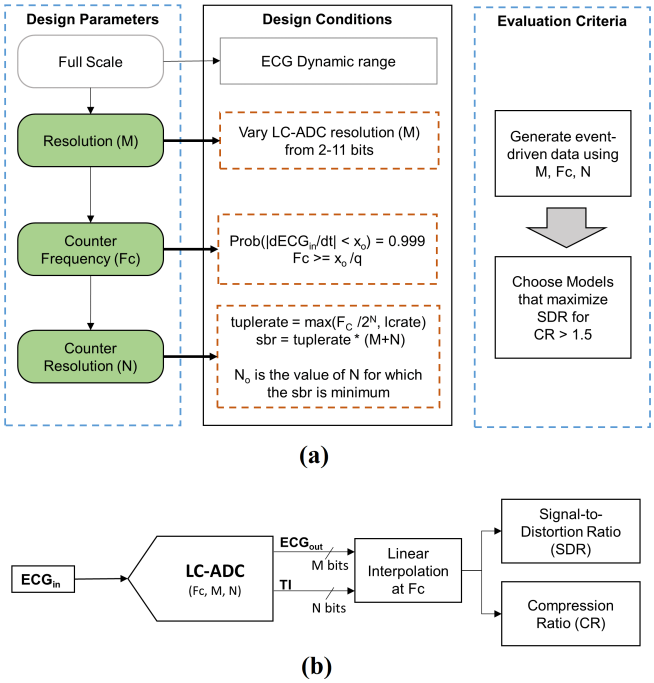

Fig. 2: (a) The proposed new methodology for selecting LC-ADC design parameters, inspired by the work presented in [3]. The three design parameters (M, N, Fc) must meet the respective design conditions before the LC-ADC can be evaluated for acceptable SDR and CR. (b) The LC-ADC evaluation methodology. ECG input is converted to event-driven signal using selected design parameters, reconstructed using linear interpolation and assessed for SDR and CR performance.

are simulated and their performance is analyzed in terms of signal quality and compression using the MIT-BIH Arrhythmia dataset [24], c) a deep learning model is proposed for event-driven cardiac arrhythmia classification and, d) an open-source event-driven ECG database derived from MIT-BIH database using the proposed LC-ADC models with arrhythmia annotations is presented.

The rest of the paper is organized as follows. Section II presents the principles of event-driven sampling for ECG applications including, LC-ADC architecture, and performance metrics for evaluation of LC-ADC models. Section III proposes a new design methodology for modeling LC-ADC parameters and evaluates several models using performance metrics. Section IV proposes a deep learning model for classification of cardiac arrhythmias using event-driven ECG data. A complexity comparison with uniformly sampled data is presented. An event-driven ECG dataset is also presented in Section IV. Finally, in Section V, conclusions are drawn.

II. Event-driven ECG Sampling

This section presents the principles of level-crossing sampling with an LC-ADC architecture and the performance metrics for compression and signal-quality evaluation of LC-ADC Models.

A. LC-ADC Architecture

The LC-ADC architecture is presented in Fig. 1a. The ECG signal range is divided into a fixed number of quantization levels. The LC-ADC sampling processing is implemented by continuously comparing against an upper and lower threshold voltage, U_QL and L_QL respectively, each of which is quantized into LSBs each having size q Volts:

$$q \triangleq \frac{A_{FS}}{2^M} \tag{1}$$

where A_{FS} is the full-scale voltage range of the ECG signal, M is the resolution of the LC-ADC and 2^M is the total number of quantization levels. The dynamic range of 10mVpp is used as the full-scale voltage throughout this study, which ensures industry standard of ambulatory equipment [3] and matches

This article has been accepted for publication in a future issue of this journal, but has not been fully edited. Content may change prior to final publication. Citation information: DOI 10.1109/TBCAS.2021.3136206, IEEE Transactions on Biomedical Circuits and Systems

the dynamic range of the MIT-BIH Arrhythmia dataset [18] used to evaluate models in this study. The difference between the upper and lower threshold voltages, Δv, is usually a fixed integer number of LSBs:

$$\Delta v = k * q \tag{2}$$

where $k \geq 1 \in \mathbb{Z}$. Typically $k = 1$, but for higher resolution LC-ADCs k is often larger so as to maintain a Δv that is greater than the noise thereby avoiding excessive threshold crossings.

Whenever the ADC's input signal crosses U_QL a sample is taken, i.e. we set ECG_{out} = U_QL and both threshold are increased by q Volts (i.e. +1 LSB). Similarly when L_QL is crossed we set ECG_{out} = L_QL and decrease the two thresholds by q Volts (i.e. -1 LSB). The control logic block in Fig. 1 manages this process. This way, an LC-ADC creates continuous-in-time discrete-in-amplitude ECG signals.

Compared to a uniform sampling ADC where the time-stamp associated with each sample is implicit, a LC-ADC however must output both the amplitude level ECG_{out} and the associated time, or equivalently the Time Interval (TI) between each sample, as a tuple $(ECG_{out}, TI)_n$, where n is an index meaning the n^{th} tuple in time. In practice the Time Interval TI is quantized w.r.t. a clock having frequency F_c and is represented using an N bit word. Whenever the Time Interval counter rolls-over, i.e. after $\frac{(2^N-1)}{F_c}$ sec during which time there were no level crossing events, an extra sample is output where the previous amplitude is simply repeated.

Using a 7-bit LC-ADC, the analog ECG signal (ECG_{in}) with event-driven samples (ECG_{out}) are presented in Fig. 1b. The horizontal grid lines represent the quantization levels spaced at q volts. The gray highlighted region on the third QRS peak is further illustrated in Fig. 1c with an LSB size of Δv = 3q volts. While the distance between U_QL and L_QL is always maintained at 3q volts, whenever a threshold crossing occurs, the two thresholds are increased or decreased by 1q volts only. Furthermore, it is worth noting the difference in time intervals between the six event-driven samples illustrated in Fig. 1c.

B. Performance metrics

To measure the signal distortion and compression in the LC-ADC output, its output samples are interpolated using linear interpolation to reconstruct the ECG signal, as in [3]. The two performance parameters are as follows:

1) *Compression Ratio (CR):* The compression ratio is the ratio of the average number of bits/sec in the signal obtained from a uniform ADC to the average number of bits/sec in the signal obtained from a LC-ADC.
2) *Signal-to-Distortion Ratio (SDR):* The temporal signal-to-distortion ratio evaluates the distortion between the original signal, x, and the reconstructed signal, $\hat{x}$ is defined as:

$$\text{SDR} = 10\log_{10}\left(\overline{(x-\bar{x})^2}\right) - 10\log_{10}\left(\overline{(x-\hat{x})^2}\right) \tag{3}$$

having units of decibels (dB).

In [25], the clinically acceptable values for SDR in ECG signal reconstruction are also reported. "Good" quality signals must follow the following criteria:

$$SDR \geq 21dB \tag{4}$$

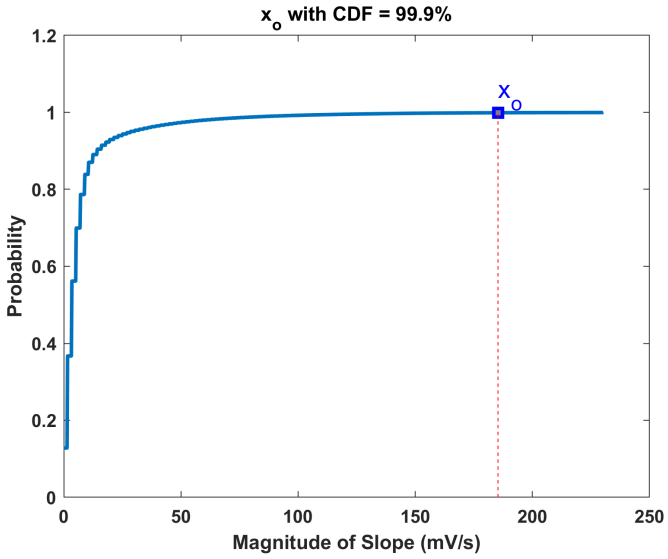

Fig. 3: The CDF of magnitude of slopes in the MIT-BIH dataset with x_o shown at 99.9%.

III. Level-crossing ADC Modeling and Evaluation

This section presents a new LC-ADC design and evaluation methodology. In order to accurately model an LC-ADC, the following design parameters must be considered: the resolution of the LC-ADC, M, the counter clock frequency, Fc, and the counter clock resolution N. These parameters simultaneously impact the sampling accuracy of the level-crossing ADC as well as accurate time tracking between two consecutive event-driven samples. First, the resolution, M, maps the number of quantization levels (2^M) in the LC-ADC. If M is too high, too many level-crossings are triggered which might produce more data than an SAR ADC [9]. If M is too low, important level-crossings will be missed and the signal-to-distortion ratio will be significantly decreased. For a fair evaluation, in this section, we design and evaluate ten LC-ADC models using resolutions $M = 2, 3, \ldots, 11$, respectively. For each of these resolutions, the ideal counter frequency and counter resolution are modeled as presented in the following subsections.

A. Selecting the Counter Clock Frequency

The fastest signal variations in ECG signals can be seen around the QRS complex as shown in Fig. 1b. In fact, these amplitude variations are larger in ECG signals with pathological abnormalities than normal conditions. The counter clock frequency should be able to keep up with these fast amplitude variations between two consecutive LC-ADC samples. Violation of this condition will lead to clipped shapes in the QRS complex [3]. Furthermore, Fc should also be fast

This article has been accepted for publication in a future issue of this journal, but has not been fully edited. Content may change prior to final publication. Citation information: DOI 10.1109/TBCAS.2021.3136206, IEEE Transactions on Biomedical Circuits and Systems

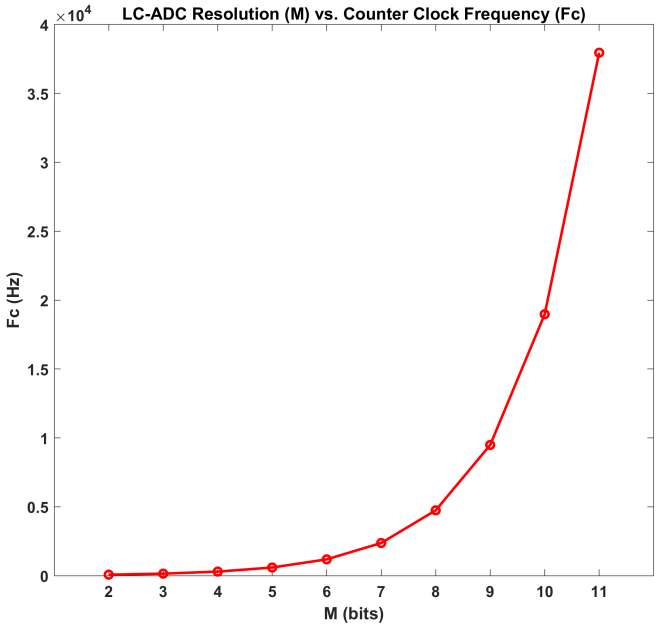

Fig. 4: Minimum Fc required to accurately model event-driven data at different LC-ADC resolutions (M).

enough to minimize time-quantization errors in mapping TI as described in Section IIA. In [3], a maximal slope condition is used to determine Fc. In general the maximal obtained from any random sample can be a statistically unreliable measure and could lead to significant over or under estimates of the typical maximum which is what, we argue, one should design according to. Thus the approach we adapt here is to estimate the CDF (Cumulative Distribution Function) of the ECG slopes and take the 99.9% level as being a reliable estimate of the typical maximum slope.

Consider the vector $\vec{x}$ containing the magnitude of slopes in the entire MIT-BIH arrhythmia dataset. Through a cumulative distributive function, find the value, x_o, in $\vec{x}$, for which the magnitude of slopes in the dataset are less than or equal to x_o, 99.9% of the time. Therefore, x_o and corresponding Fc can be calculated as:

$$\mathrm{P}\left(\left|\frac{\mathrm{d}ECG_{in}}{\mathrm{d}t}\right| \leq x_o\right) \simeq 0.999 \tag{5}$$

$$\Rightarrow Fc \geq \frac{x_o}{q} \tag{6}$$

Fig. 3 shows the cumulative distributive function of magnitude of slopes in the MIT-BIH dataset with x_o shown at 99.9%. Fig. 4 shows the value of F_c obtained in this manner as a function of the LC-ADC resolution (M) obtained by simulation over the entire MIT-BIH Arrhythmia dataset. These result are also summarized in Section IIIC, Table I. As M is increased, the LSB size, q decreases, thereby increasing the counter clock frequency required to capture fast slopes in the ECG signal. At M = 8 bits, the minimum required Fc is 4744.24Hz, which is less than half of that used in [3] for the same LC-ADC resolution.

B. Determining the Counter Clock Resolution

Lastly, the final design parameter, counter clock resolution (N), directly impacts the number of bits per second generated by the LC-ADC, defined as the stream-bit-rate (sbr). Mostly, sbr is dominated by the level-crossing rate ($lcrate$), which is the average sampling rate (i.e. the average level crossing rate) of the LC-ADC. However, as described in Section IIA, the LC-ADC design presented in this study can also output a tuple at every clock rollover i.e, every $\frac{(2^N-1)}{F_c}$ seconds if there has been no level crossing during this time[1]. If N is chosen to be very small, too many tuples are generated. Similarly, if N is too high, the size of TI (N-bit word) will be large. In other words, the number of bits per tuple increases linearly as N is increased. It is worth noting that this approach does not add any additional overhead in terms of the tuple transfer rate as it occurs quite infrequently. We propose to find the optimal value of N for which the sbr is minimum. The sbr can be defined as,

$$\text{tuple\_rate} = \max\left(\frac{Fc}{2^N}, \text{lcrate}\right) \tag{7}$$

$$sbr = \text{tuple\_rate} * (M + N) \tag{8}$$

We simulated sbr over $N = 3, 4, \ldots, 16$ using the resolutions, M and counter clock frequency, Fc, pairs estimated in the previous subsections. Fig. 5 shows the sbr for varying counter clock resolution (N) over different LC-ADC resolutions (M). In each sub-figure, the optimal choice of N for which sbr is minimum is marked as N_o. It can be observed that as N grows large, sbr grows linearly. When M and N are both small, sbr is large due the tuple_rate being dominated by the clock roll-over samples. When M is large enough, however, tuple_rate is dependent on the LSB size. Fig. 6 summarizes the optimal N choice for each resolution of the LC-ADC. It can be observed that when M is big enough and the sbr is largely dependent on the LSB size (q), the counter clock resolution (N) does not need to be too large. However, when M is small, N must be chosen higher so as not to generate too many tuples from counter clock roll-over.

In the next subsection, the three chosen design parameters, i.e. counter clock frequency (Fc) and counter clock resolution (N) for each LC-ADC resolution (M) are evaluated for compression performance and signal quality.

C. Evaluation of LC-ADC Models

The LC-ADC design parameters and the respective design conditions they must meet are summarized in Fig. 2a. It also presents the LC-ADC evaluation criteria using the two performance metrics, compression ratio (CR) and signal-to-distortion ratio (SDR), introduced in Section IIB. These can help designers choose the right LC-ADC model for their application. Fig 2b shows the LC-ADC evaluation methodology used in this subsection. We converted the 48 recordings in

[1]Other design options include increasing N such that the smallest slope in the ECG signal can be captured or to add an overflow flag in the hardware design. However, these would add further complexity in the downstream processing. Repeating a tuple is a simpler solution which adds very little complexity.

This article has been accepted for publication in a future issue of this journal, but has not been fully edited. Content may change prior to final publication. Citation information: DOI 10.1109/TBCAS.2021.3136206, IEEE Transactions on Biomedical Circuits and Systems

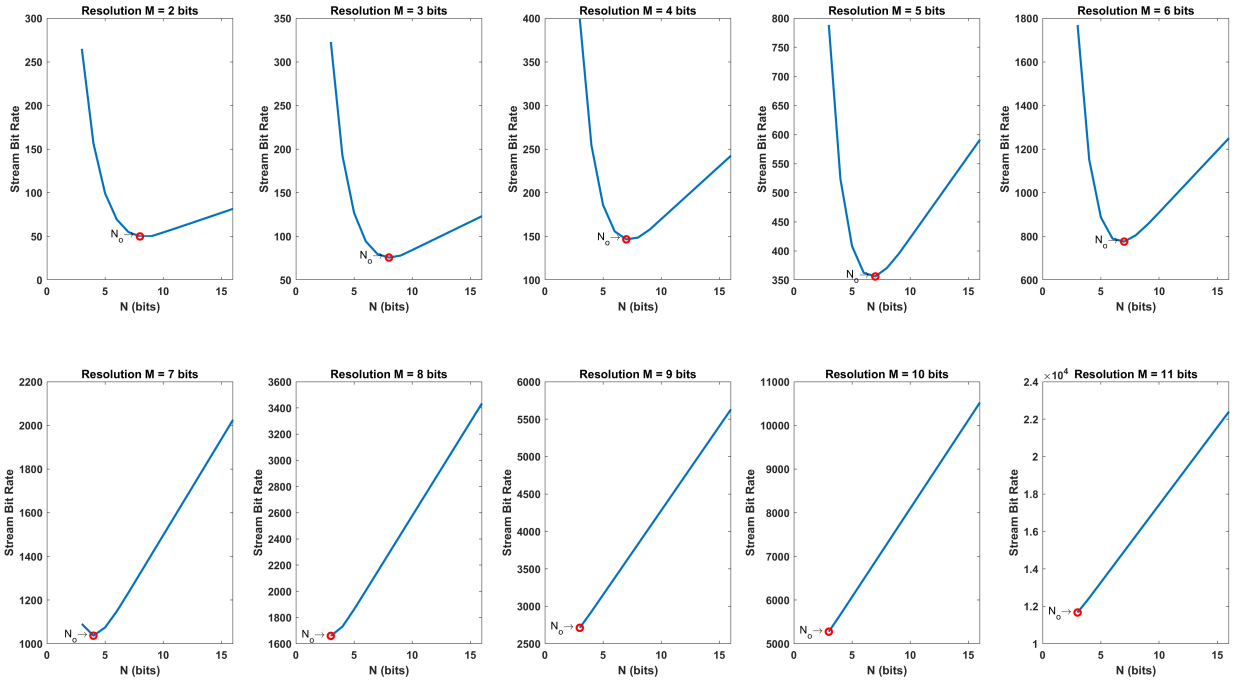

Fig. 5: The stream-bit-rate for varying counter clock resolution (N) over different LC-ADC resolutions (M).

TABLE I: Compression and Signal Quality Analysis of LC-ADC Models

M	Fc (Hz)	N	CR	SDR (dB)
2	74.13	8	83.96	-2.93
3	148.26	8	60.04	-1.10
4	296.51	7	30.34	2.72
5	593.03	7	13.11	9.06
6	1186.06	7	6.46	15.61
7	2372.12	4	1.59	19.91
8	4744.24	3	0.46	24.94
9	9488.49	3	0.23	29.92
10	18976.97	3	0.12	34.54
11	37953.94	3	0.06	38.68

the MIT-BIH Arrhythmia dataset to event-driven data using the ten (M, Fc, N) value sets summarized in Table I, then reconstructed the signals to Fc using linear interpolation and evaluated them using CR and SDR. The aim is to select LC-ADC models that maximize the SDR subject to a CR greater than 1.5.

Fig. 7 shows the compression ratio at different resolutions of M. A CR of 1 indicates no compression, while for CR $\leq$ 1, the LC-ADC model generates more samples than a Nyquist Sampling ADC. A compression ratio greater than 1.5 would indicate acceptable compression. It can be observed that for M $>$ 7 bits, the CR is less than 1, which means a Nyquist sampling ADC will be better for high-resolution applications. For models with M $\leq$ 7, good compression can be observed.

Ideally, an LC-ADC must maximize the SDR for a given CR. We extend this condition to also include the signal quality criteria presented in eq. (4). However, it must be noted that for some ECG applications, an SDR less than 21dB might also be acceptable. Fig. 8 shows the SDR at different resolutions of M. The models with M $\geq$ 7 have SDR close to the 21dB criteria. However, the most promising trade-off between CR and SDR can be observed at M = 7. To study this LC-ADC resolution further, we looked into varying the counter clock resolution (N). The MIT-BIH Arrhythmia dataset is originally sampled at 360Hz using an 11-bit ADC. In order, to sample close to the Fc of 2372.12 Hz for M= 7 bits, we first up-sample the entire database to 38160Hz. From this up-sampled database, we then sample at Fc = 2385Hz, which is 0.54% greater than the minimum required Fc at this resolution. Then using M= 7 bits and Fc = 2385Hz, we varied N from 4 to 8-bits to search over the curve created with these values (see M=7 bits in Fig. 5). Beyond 8-bit counter clock resolution, the sbr starts increasing linearly and therefore, excluded from analysis here. The results are summarized in Table II.

In all N we simulated the case where the step-size between the two LC-ADC thresholds, Δv, was set to q (i.e. 1 LSB) but additionally for the N = 6 to 8 bits models were also evaluated at $\Delta v = 2q$ as they have SDR $>$ 21dB. From the eight models summarized in this table, MDL6, MDL7, and MDL8 follow the criteria of eq. (4). However, MDL8 gives the most ideal CR and SDR trade-off at a slightly higher sbr of 1320.92 bps. Moreover, MDL4, MDL5, and MDL6b, MDL7b, and MDL8b with $\Delta v = 2q$ might still be acceptable for certain applications with SDR $>$ 20dB. All of these models are evaluated for event-driven arrhythmia classification in the following section.

IV. Cardiac Arrhythmia Classification using Event-Driven ECG

In this section, a new deep learning based classifier is presented and the eight LC-ADC models summarized in Ta-

This article has been accepted for publication in a future issue of this journal, but has not been fully edited. Content may change prior to final publication. Citation information: DOI 10.1109/TBCAS.2021.3136206, IEEE Transactions on Biomedical Circuits and Systems

TABLE II: Compression and Signal Quality Analysis of LC-ADC Models at M = 7 bits and Fc = 2385 Hz

Model	N	LSB	CR	SDR (dB)	sbr (bps)
MDL4	4	q	1.59	19.91	1036.82
MDL5	5	q	2.34	20.46	1074.44
MDL6	6	q	2.92	21.19	1147.75
MDL7	7	q	3.25	21.99	1233.14
MDL8	8	q	3.38	22.57	1320.92
MDL6b	6	2q	3.66	20.66	-
MDL7b	7	2q	4.45	20.75	-
MDL8b	8	2q	4.94	20.25	-

ble II are analyzed for event-driven ECG classification. Then, a complexity analysis in terms of floating point operations per second for each model is presented and a comparison is made with uniformly sampled data. Lastly, an open-source event-driven ECG dataset is summarized based on the best performing LC-ADC models from this study.

A. *Deep Learning Based Classifier*

We designed a one-dimensional convolutional neural network as illustrated in Fig. 9. This 1D-CNN model has three convolutional layers followed by two fully-connected layers. Each convolutional layer has 64 filters of size 3, each. A stride of 1 is maintained throughout the network. Batch normalization and max pooling is applied after each convolutional layer to accelerate training and to reduce over-fitting. Max pooling also helps reduce complexity of the network in subsequent layers. To further ensure that over-fitting is minimized a dropout of 50% probability is applied between the two fully connected layers. Sparse categorical cross-entropy is used as the loss function with an ADAM optimizer and a learning rate of 0.001. The exponential decay rate for the 1st and 2nd moment estimates is set to 0.9 and 0.99, respectively.

The size of the input layer varies for each model based on the number of features. The output layer uses a softmax layer and classifies each beat into one of the following four categories: normal beat (N), supraventricular ectopic beats (S), ventricular ectopic beats (V), and fusion beats (F). The prominent morphological features of an ECG beat is contained in approximately an 800ms window [12] centered around the QRS peak as shown in Fig. 1b. For every model, we take

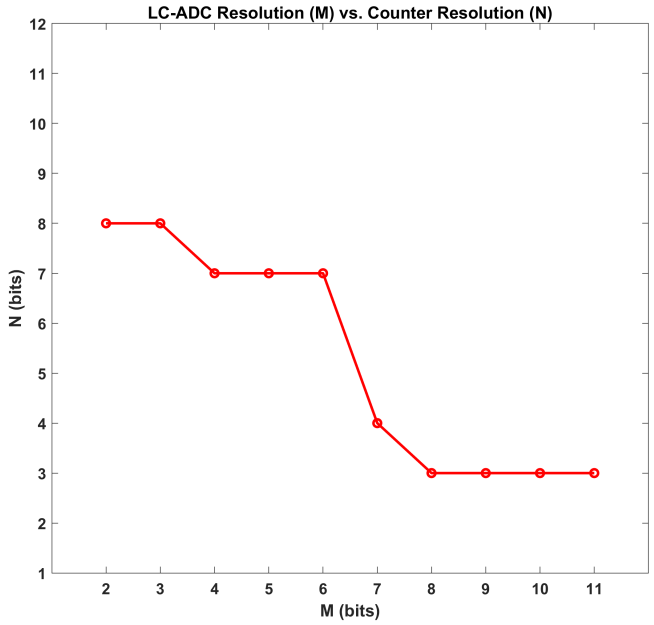

Fig. 6: Counter clock resolution (N) that minimizes the stream-bit-rate over different LC-ADC resolutions (M).

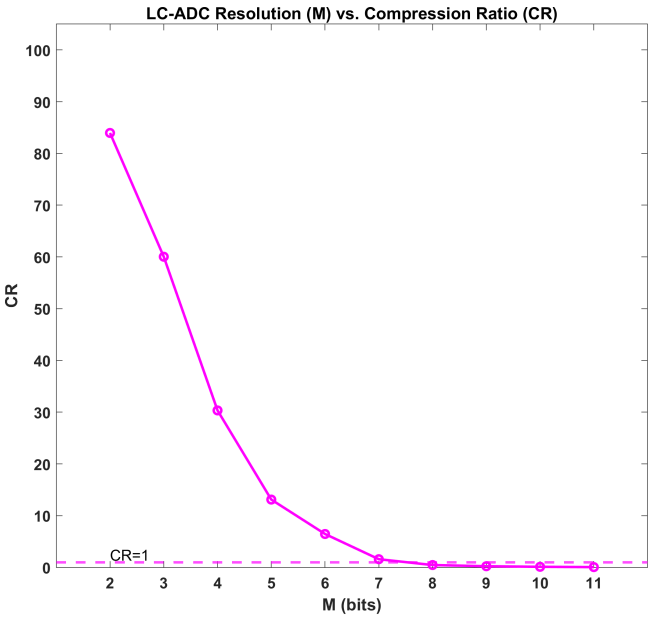

Fig. 7: The compression ratio (CR) over the different LC-ADC resolutions (M). A CR of 1 represents no compression.

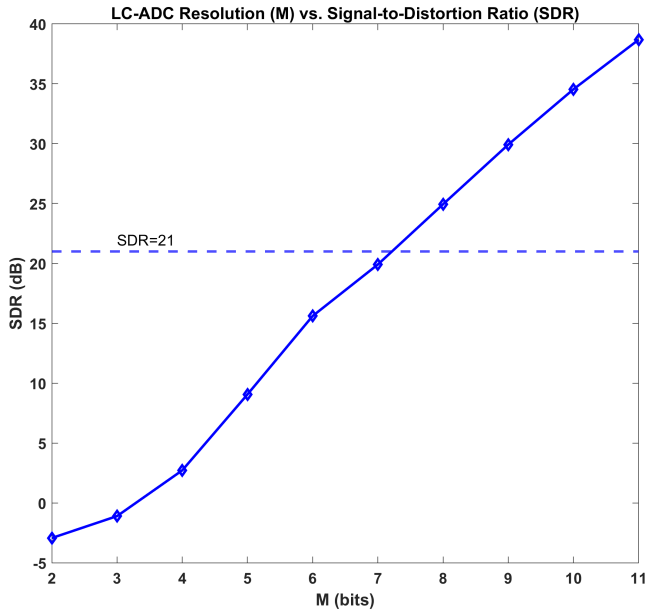

Fig. 8: SDR vs LC-ADC resolutions (M). SDR = 21dB represents the cross over line for 'good' quality signals.

This article has been accepted for publication in a future issue of this journal, but has not been fully edited. Content may change prior to final publication. Citation information: DOI 10.1109/TBCAS.2021.3136206, IEEE Transactions on Biomedical Circuits and Systems

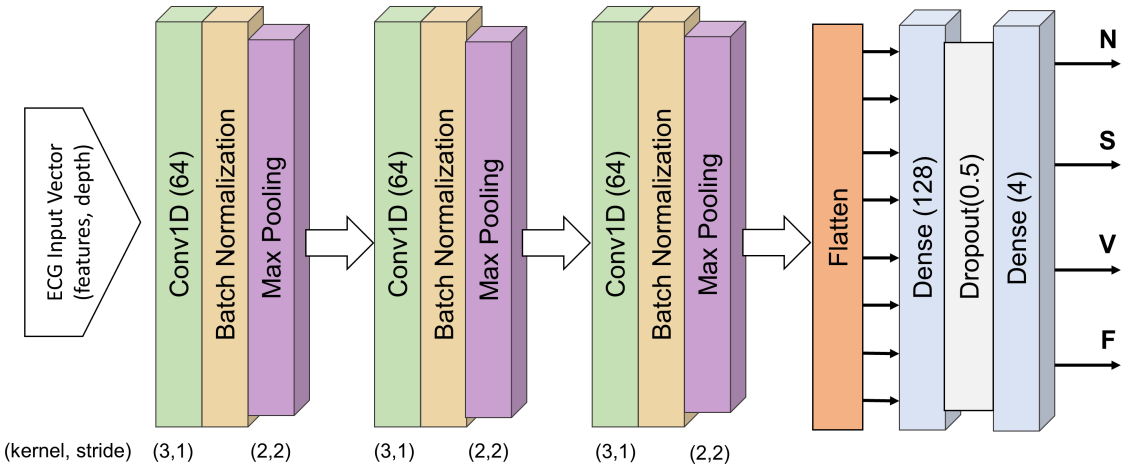

Fig. 9: Proposed one-dimensional CNN for event-driven ECG classification

300ms before the R peak and 400ms after the R peak as a feature set, the size of which is indicated by $features$ variable of the input vector in Fig. 9. For event-driven models, a second channel containing time at each sample relative to the R peak is added. The number of channels are indicated as $depth$ of the input vector in Fig. 9. Finally, to handle the extreme class-imbalance inherent in the dataset, we use Synthetic Minority Oversampling TEchnique (SMOTE) to statistically balance the training set.

B. Classification Performance

A global training and verification approach is applied for classification of arrhythmias in the MIT-BIH Arrhythmia dataset. The four paced records 102, 104, 107 and 217 are excluded from the analysis as recommended by the Association for the Advancement of Medical Instrumentation (AAMI) [26]. All the beats from the remaining records are split into 65% training set, 10% validation set, and 25% test set. For a fair comparison, we have also tested the classifier on uniformly-sampled data using the MIT-BIH database as is, named MDL0 from here on. The MIT-BIH database is sampled at 360Hz using an 11-bit ADC. Since time information is implicit in uniformly sampled data, we only use the amplitudes at each sample as input to the 1D-CNN. The input feature vector for the uniform model is of the size 238x1 (features, depth). While, all event-driven models have an input vector size of 120x2 (features, depth). Accuracy (ACC), sensitivity (SEN), positive predictivity (+PV), and false positive rate (FPR) are used to assess the classifier performance and are defined as follows:

$$ACC = \frac{(TP + TN)}{(TP + FP + FN + TN)} \tag{9}$$

$$SEN = \frac{TP}{(TP + FN)} \tag{10}$$

$$+PV = \frac{TP}{(TP + FP)} \tag{11}$$

$$FPR = \frac{FP}{(FP + TN)} \tag{12}$$

where TP, TN, FP, and FN are the number of true positives, true negatives, false positive and false negatives per class. The classification results for each using the eight event-driven models and the uniformly sampled, MDL0, are summarized in Table III. The classification performance of MDL0 is the benchmark for comparison with ACC, SEN and +PPV, all above 92%. In terms of overall performance considering all four classification parameters, MDL5 has the closest performance to MDL0. This is closely followed by MDL7b, MDL4 and MDL6b. If overall sensitivity is considered, MDL6b and MDL5 at 89.99% and 89.98% SEN, respectively, are closest in performance to MDL0. The overall sensitivity performance of event-driven models can be further improved by using a better class-balancing technique. Next, the overall +PV is greater than 90% for all event-driven models except MDL8b, while the FPR is lowest for MDL5 from all event-driven models. Classification performance by itself is not a good indicator for evaluation of event-driven models. We must also consider the complexity, therefore, we now present complexity analysis in the next subsection.

C. Accuracy-Complexity Trade-off

Table IV summarizes the complexity analysis of event-driven and uniformly sampled 1D-CNN models. Since all event-driven models summarized in Table II use an LC-ADC resolution of 7 bits, their feature sets can be roughly captured in 120 features with 2 channels (depth). Therefore, the number of trainable parameters for the 1D-CNN classifier are consistently 132,676 for all event-driven models. The uniformly sampled model takes 238 features with 1 channel (depth), yet the number of trainable parameters are doubled at 255,748 compared to the event-driven models. We also calculated the number of floating point operations per second (FLOPS) required by the event-driven and uniformly sampled models. The uniformly sampled model requires 4883224 FLOPS, while the event-driven models only require 49% of this at 2397144 FLOPS. As expected, the uniformly sampled model has superior classification performance compared to all event-driven models.

This article has been accepted for publication in a future issue of this journal, but has not been fully edited. Content may change prior to final publication. Citation information: DOI 10.1109/TBCAS.2021.3136206, IEEE Transactions on Biomedical Circuits and Systems

TABLE III: Arrhythmia Classification Summary

Model	Class	ACC	SEN	+PV	FPR
MDL0	N	99.09	99.59	99.40	5.10
	S	99.45	86.97	92.46	0.20
	V	99.65	97.73	97.29	0.20
	F	99.80	85.71	90.00	0.08
	Average	**99.49**	**92.40**	**94.78**	**1.39**
MDL4	N	98.39	99.48	98.72	10.87
	S	98.94	72.65	86.55	0.32
	V	99.49	94.85	97.84	0.16
	F	99.75	82.86	86.57	0.11
	Average	**99.14**	**87.46**	**92.42**	**2.86**
MDL5	N	98.53	99.20	99.14	7.19
	S	99.03	81.48	83.04	0.47
	V	99.51	96.88	96.12	0.29
	F	99.76	82.38	88.26	0.09
	Average	**99.20**	**89.98**	**91.64**	**2.01**
MDL6	N	98.57	99.55	98.86	9.71
	S	99.13	76.98	90.01	0.37
	V	99.49	95.19	97.45	0.19
	F	99.74	80.48	87.56	0.10
	Average	**99.23**	**88.05**	**93.47**	**2.59**
MDL7	N	98.34	99.32	98.82	9.97
	S	98.96	75.68	84.90	0.37
	V	99.42	95.07	96.06	0.16
	F	99.69	78.51	83.33	0.13
	Average	**99.10**	**87.14**	**90.77**	**2.66**
MDL8	N	98.31	99.36	98.75	10.57
	S	98.93	76.55	83.31	0.43
	V	99.43	94.22	97.53	0.18
	F	99.71	77.61	86.70	0.10
	Average	**99.09**	**86.92**	**90.42**	**2.82**
MDL6b	N	98.50	99.20	99.12	7.42
	S	99.07	81.91	83.98	0.44
	V	99.44	95.98	96.09	0.29
	F	99.71	82.86	82.86	0.14
	Average	**99.18**	**89.99**	**90.51**	**2.07**
MDL7b	N	98.53	99.53	98.83	9.94
	S	99.13	75.40	91.24	0.20
	V	99.43	95.02	96.83	0.23
	F	99.72	81.43	84.24	0.13
	Average	**99.20**	**87.84**	**92.78**	**2.62**
MDL8b	N	98.23	99.01	99.01	8.36
	S	98.92	81.04	80.00	0.57
	V	99.37	95.13	95.89	0.31
	F	99.69	82.86	80.93	0.16
	Average	**99.05**	**89.51**	**88.95**	**2.35**

In order to better understand the accuracy-complexity trade-off in event-driven models, we have analyzed the four most important parameters for a comparative analysis, namely the classification performance and complexity of the classifier as well as the compression and the signal quality of the ECG data. Fig. 10 shows the comparison with sensitivity of all models with their respective compression ratios. The models that follow the signal quality criteria of eq. (4) are colored blue, while those that do not are colored orange. Fig. 11 and Fig. 12 present a similar comparison using accuracies and positive predictive values of all models. In terms of accuracy, in Fig. 11, MDL6 offers the best accuracy and a

TABLE IV: Complexity Analysis of Event-Driven and Uniformly Sampled 1D-CNN Models

Type	Input Vector	Parameters	FLOPS
Event-Driven	120x2	132,676	2397144
Uniform	238x1	255,748	4883224

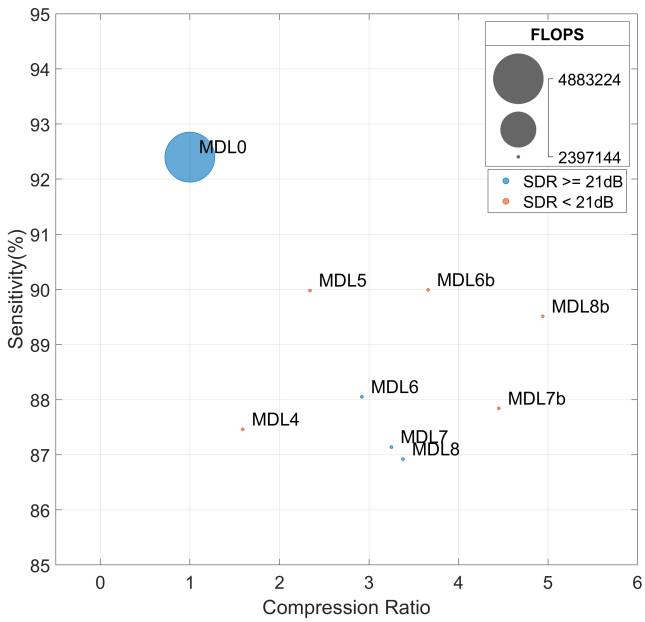

Fig. 10: Sensitivity vs CR vs FLOPS for LC-ADC models

good SDR at >21dB. This is the 7-bit model at counter clock resolution of 6 bits. MDL5 and MDL7b are close at 99.2% accuracy, while these models use N=5 with Δv=1LSB and N=7 with Δv=2LSB, respectively. Both MDL5 and MDL7 have SDR less than 21dB. Overall, MDL7b offers the best compression at 4.45 compared to the CR of 2.92 and 2.34 in MDL6 and MDL5, respectively. In this regard, considering the overall classification accuracy, MDL7b offers the best accuracy-compression-complexity trade off at SDR=20.75dB. In terms of positive predictive value, in Fig. 12, MDL6 still offers the best compression to signal-quality trade-off with excellent +PV and SDR greater than 21dB. This is closely followed by MDL4 and MDL7b, both of which have less than 21dB SDR. However, at CR=1.59, MDL4 offers the lowest compression. If higher signal compression is desired, MDL7b offers a better trade off with SDR of 20.75dB, which would still be acceptable for many applications. This higher compression can be attributed to the larger step-size between the upper and lower thresholds of the LC-ADC. It must be noted that higher compression rates imply lesser sampling by the LC-ADC and thereby, lesser power consumption in the circuit.

For biomedical applications, sensitivity is often considered the most important parameter as the cost of a misclassified true positives is much higher than the cost of misclassified true negatives. Therefore, in terms of sensitivity of different sampling schemes presented in Fig. 10, MDL5, MDL6 and MDL8b offer the best classification-compression trade off. All

This article has been accepted for publication in a future issue of this journal, but has not been fully edited. Content may change prior to final publication. Citation information: DOI 10.1109/TBCAS.2021.3136206, IEEE Transactions on Biomedical Circuits and Systems

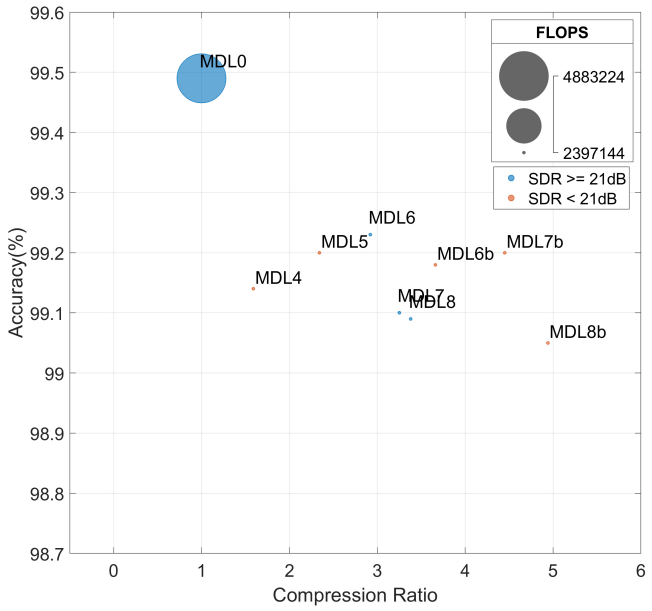

Fig. 11: Accuracy vs CR vs FLOPS for LC-ADC models

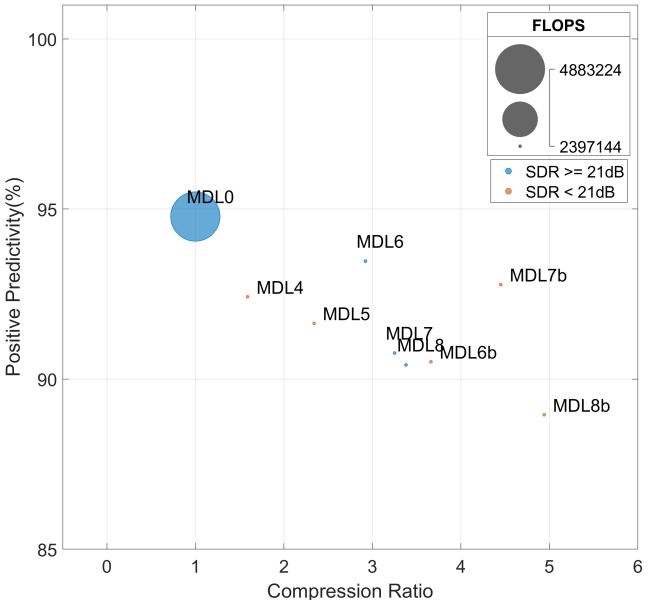

Fig. 12: Positive predictivity vs CR vs FLOPS for LC-ADC models

three of these models offer greater than 20dB SDR. With sensitivity at approximately 90%, MDL5 and MDL6 offer a compression of 2.34 and 2.93, respectively. In comparison with the uniformly sampled MDL0, MDL8b has 2.89% less SEN but offers a CR of 4.94. Overall, considering all three parameters, MDL6, offers the best performance with CR of 2.92 and SDR of 21.19. Therefore, a 7-bit LC-ADC with a 2385Hz counter clock frequency and a 6-bit counter clock resolution will offer comparative classification performance to a Nyquist ADC at 11-bits and 360Hz. The LC-ADC will save power by reducing the average sampling rate while maintaining good signal quality. Classification using the LC-ADC will require only 49% of the FLOPS required by data generated from a Nyquist sampling ADC.

D. Open-Source Event-Driven ECG Dataset

To the best of our knowledge, there is no publicly available non-uniformly sampled ECG dataset with arrhythmia labels for researching event-driven data processing and classification. Therefore, in this study, we used the popular MIT-BIH arrhythmia database and different LC-ADC models to derive a non-uniformly sampled event-driven ECG dataset. The dataset is generated using a MATLAB script and can generate LC-ADC data at different LC-ADC resolutions, clock frequencies and counter clock resolutions. The event-driven ECG dataset with arrhythmia annotations and corresponding MATLAB scripts is open-sourced in authors' website[2] to enable further research on the topic.

V. Conclusions

A new LC-ADC design and evaluation methodology was presented. For a given LC-ADC resolution, the minimum required counter clock frequency was estimated using the standard deviation means of 99.9 percentile magnitude of slopes. Furthermore, the counter clock resolution was chosen based on the number of bits that produce the minimum stream-bit-rate per second. The stream-bit-rate was estimated using the clock roll-over frequency, the average sampling rate of the LC-ADC and the size of the tuples generated by the LC-ADC. Using these design methodologies, ten different event-driven models were analyzed in terms of compression and signal-to-distortion ratio. Since the 7-bit LC-ADC model offered the best compression and signal-quality, this model was further analyzed at different counter clock resolutions and different gaps between the LC-ADC thresholds. Then, a new 1D-CNN model was presented for cardiac arrhythmia classification. The event-driven models and a uniformly sampled model was analyzed for classification performance using the 1D-CNN. Then a thorough accuracy-complexity analysis was presented. It was concluded that a 7-bit LC-ADC at 2385Hz counter clock frequency and a 6-bit counter clock resolution offers the best accuracy-compression-complexity trade off. With classification performance comparable to a Nyquist sampled ADC, this LC-ADC model offers 3x data compression while maintaining the signal-to-distortion ratio of more than 21dB. Furthermore, this model requires only 49% FLOPS for classification in comparison with a uniformly sampled model. Therefore, the new LC-ADC evaluation and design methodology presented in this paper is a good tool for designers to choose an appropriate LC-ADC model for their event-driven applications, which may not be limited to ECG data. Finally, we developed an open-source event-driven ECG database with arrhythmia annotations for enabling further research on non-uniformly sampled data processing.

[2]The open-source event-driven ECG dataset is available at https://github.com/jedaiproject/Open-Source-Event-Driven-ECG-Dataset

This article has been accepted for publication in a future issue of this journal, but has not been fully edited. Content may change prior to final publication. Citation information: DOI 10.1109/TBCAS.2021.3136206, IEEE Transactions on Biomedical Circuits and Systems

REFERENCES

[1] D. L. T. Wong, J. Yu, Y. Li, C. J. Deepu, D. H. Ngo, C. Zhou, S. R. Singh, A. Koh, R. Hong, B. Veeravalli, M. Motani, K. C. Chua, Y. Lian, and C. Heng, "An integrated wearable wireless vital signs biosensor for continuous inpatient monitoring," *IEEE Sensors Journal*, vol. 20, no. 1, pp. 448–462, 2020.

[2] F. Chen, F. Lim, O. Abari, A. Chandrakasan, and V. Stojanovic, "Energy-aware design of compressed sensing systems for wireless sensors under performance and reliability constraints," *IEEE Transactions on Circuits and Systems I: Regular Papers*, vol. 60, no. 3, pp. 650–661, 2013.

[3] M. Tlili, M. Ben-Romdhane, A. Maalej, F. Rivet, D. Dallet, and C. Rebai, "Level-crossing ADC design and evaluation methodology for normal and pathological electrocardiogram signals measurement," *Measurement*, vol. 124, pp. 413–425, 2018.

[4] Y. Yin, S. M. Abubakar, S. Tan, J. Shi, P. Yang, W. Yang, H. Jiang, Z. Wang, W. Jia *et al.*, "A 2.63 w ecg processor with adaptive arrhythmia detection and data compression for implantable cardiac monitoring device," *IEEE Transactions on Biomedical Circuits and Systems*, 2021.

[5] J. Li, A. Ashraf, B. Cardiff, R. C. Panicker, Y. Lian, and D. John, "Low power optimisations for iot wearable sensors based on evaluation of nine qrs detection algorithms," *IEEE Open Journal of Circuits and Systems*, vol. 1, pp. 115–123, 2020.

[6] C. J. Deepu, X. Y. Xu, D. L. T. Wong, C. H. Heng, and Y. Lian, "A 2.3 μ w ecg-on-chip for wireless wearable sensors," *IEEE Transactions on Circuits and Systems II: Express Briefs*, vol. 65, no. 10, pp. 1385–1389, 2018.

[7] F. Corradi, S. Pande, J. Stuijt, N. Qiao, S. Schaafsma, G. Indiveri, and F. Catthoor, "Ecg-based heartbeat classification in neuromorphic hardware," in *2019 International Joint Conference on Neural Networks (IJCNN)*. IEEE, 2019, pp. 1–8.

[8] C. J. Deepu, X. Zhang, C. H. Heng, and Y. Lian, "A 3-lead ecg-on-chip with qrs detection and lossless compression for wireless sensors," *IEEE Transactions on Circuits and Systems II: Express Briefs*, vol. 63, no. 12, pp. 1151–1155, 2016.

[9] J. Van Assche and G. Gielen, "Power Efficiency Comparison of Event-Driven and Fixed-Rate Signal Conversion and Compression for Biomedical Applications," *IEEE Transactions on Biomedical Circuits and Systems*, vol. 14, no. 4, pp. 746–756, 2020.

[10] T. Marisa, T. Niederhauser, A. Haeberlin, R. A. Wildhaber, R. Vogel, J. Goette, and M. Jacomet, "Pseudo asynchronous level crossing adc for ecg signal acquisition," *IEEE transactions on biomedical circuits and systems*, vol. 11, no. 2, pp. 267–278, 2017.

[11] X. Zhang and Y. Lian, "A 300-mV 220-nW Event-Driven ADC With Real-Time QRS Detection for Wearable ECG Sensors," *IEEE Transactions on Biomedical Circuits and Systems*, vol. 8, no. 6, pp. 834–843, 2014.

[12] Y. Zhao, Z. Shang, and Y. Lian, "A 13.34 μW Event-Driven Patient-Specific ANN Cardiac Arrhythmia Classifier for Wearable ECG Sensors," *IEEE Transactions on Biomedical Circuits and Systems*, vol. 14, no. 2, pp. 186–197, 2019.

[13] Y. Li, D. Zhao, and W. A. Serdijn, "A sub-microwatt asynchronous level-crossing adc for biomedical applications," *IEEE Transactions on Biomedical Circuits and Systems*, vol. 7, no. 2, pp. 149–157, 2013.

[14] Y. Hou *et al.*, "A 61-nW level-crossing ADC with adaptive sampling for biomedical applications," *IEEE Transactions on Circuits and Systems II: Express Briefs*, vol. 66, no. 1, pp. 56–60, 2018.

[15] Y. Hou, K. Yousef, M. Atef, G. Wang, and Y. Lian, "A 1-to-1-khz, 4.2-to-544-nw, multi-level comparator based level-crossing adc for iot applications," *IEEE Transactions on Circuits and Systems II: Express Briefs*, vol. 65, no. 10, pp. 1390–1394, 2018.

[16] C. Weltin-Wu and Y. Tsividis, "An event-driven clockless level-crossing ADC with signal-dependent adaptive resolution," *IEEE Journal of Solid-State Circuits*, vol. 48, no. 9, pp. 2180–2190, 2013.

[17] K. Kozmin, J. Johansson, and J. Delsing, "Level-crossing adc performance evaluation toward ultrasound application," *IEEE Transactions on Circuits and Systems I: Regular Papers*, vol. 56, no. 8, pp. 1708–1719, 2008.

[18] N. Ravanshad *et al.*, "A Level-Crossing Based QRS-Detection Algorithm for Wearable ECG Sensors," *IEEE Journal of Biomedical and Health Informatics*, vol. 18, no. 1, pp. 183–192, 2014.

[19] A. Darwish, L. Fesquet, and G. Sicard, "1-level crossing sampling scheme for low data rate image sensors," in *2014 IEEE 12th International New Circuits and Systems Conference (NEWCAS)*. IEEE, 2014, pp. 289–292.

[20] Z. Wang, Y. Liu, P. Zhou, Z. Tan, H. Fan, Y. Zhang, L. Shen, J. Ru, Y. Wang, L. Ye *et al.*, "A 148-nw reconfigurable event-driven intelligent wake-up system for aiot nodes using an asynchronous pulse-based feature extractor and a convolutional neural network," *IEEE Journal of Solid-State Circuits*, 2021.

[21] Y. Wei, J. Zhou, Y. Wang, Y. Liu, Q. Liu, J. Luo, C. Wang, F. Ren, and L. Huang, "A review of algorithm & hardware design for ai-based biomedical applications," *IEEE transactions on biomedical circuits and systems*, vol. 14, no. 2, pp. 145–163, 2020.

[22] S. K. Cherupally, S. Yin, D. Kadetotad, G. Srivastava, C. Bae, S. J. Kim, and J.-s. Seo, "Ecg authentication hardware design with low-power signal processing and neural network optimization with low precision and structured compression," *IEEE transactions on biomedical circuits and systems*, vol. 14, no. 2, pp. 198–208, 2020.

[23] M. Saeed, Q. Wang, O. Märtens, B. Larras, A. Frappé, B. Cardiff, and D. John, "Event-driven ecg classification using an open-source, lc-adc based non-uniformly sampled dataset," in *2021 IEEE International Symposium on Circuits and Systems (ISCAS)*. IEEE, 2021, pp. 1–5.

[24] A. L. Goldberger *et al.*, "Physiobank PhysioToolkit and PhysioNet components of a new research resource for complex physiologic signals," *Circulation*, vol. 101, no. 23, pp. e215–e220, 2000.

[25] Y. Zigel *et al.*, "The weighted diagnostic distortion (WDD) measure for ECG signal compression," *IEEE transactions on biomedical engineering*, vol. 47, no. 11, pp. 1422–1430, 2000.

[26] A.-A. EC57, A. for the Advancement of Medical Instrumentation *et al.*, "Testing and reporting performance results of cardiac rhythm and ST segment measurement algorithms," *Association for the Advancement of Medical Instrumentation, Arlington, VA*, 1998.

Maryam Saeed received her M.S. degree in Electrical Engineering from National University of Sciences and Technology, Islamabad and her B.S. in Telecommunication Engineering from the National University of Computer and Emerging Sciences, Lahore. She is a PhD scholar at the University College Dublin and a Schlumberger Faculty for the Future Fellow. Her current research includes designing arrhythmia classifiers for low power circuits using event-driven ADCs.

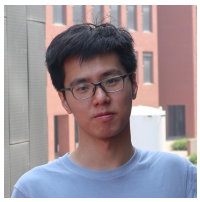

Qingyuan Wang received the B.E degree with the first honor from both University College Dublin (UCD) and Beijing University of Technology (BJUT) in 2019. He is working towards a Ph.D. degree with SFI Centre for Research Training in Machine Learning at UCD. His interests include deep learning and its implementation on hardware.

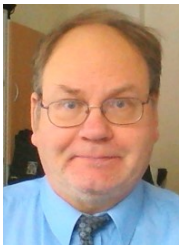

Olev Martens (Senior member, IEEE) has born in Tallinn, Estonia, 1960. Dipl. engineer of electronics (CUM LAUDE) from 1983, PhD from 2000, both degrees from Tallinn University of Technology (TalTech). He has experience in the industrial R&D, and from 2000 in academy, being senior and lead researcher and now associate professor of measurement electronics at Thomas Johann Seebeck Department of Electronics, TalTech.

This article has been accepted for publication in a future issue of this journal, but has not been fully edited. Content may change prior to final publication. Citation information: DOI 10.1109/TBCAS.2021.3136206, IEEE Transactions on Biomedical Circuits and Systems

Benoit Larras was born in Nancy, France in 1988. He received both his engineering degree and his Master in Telecommunications from IMT Atlantique in 2012. He received his Ph.D. in Electrical Engineering in 2015 from IMT Atlantique, Brest, France. He is now an associate professor at Junia, Lille, France, in the Electronics Team. His research topic is about analog/mixed-signal IC design and circuit implementation of neural networks and associative memories, in the context of "Near-sensor computing" and "Edge computing". He is the co-recipient of a Best Paper at the IEEE AICAS2020 conference.

Antoine Frappe (M'08-SM'17) graduated from the Institut Supérieur d'Electronique du Nord (ISEN), Lille, France in 2004. He received the M.Sc., Ph.D., and HDR (French highest academic degree) in electrical engineering from the University of Lille, France in 2004, 2007, and 2019, respectively. Since 2004, he is a member of the Silicon Microelectronics group at the Institute of Electronics, Microelectronics, and Nanotechnologies (IEMN) in Villeneuve d'Ascq, France. He obtained a Fulbright grant in 2008 to pursue research in communication systems at the Berkeley Wireless Research Center (BWRC) at UC Berkeley, CA, USA. He is now an Associate Professor at Junia ISEN, Lille, France, leading the Electronics Team. His research interests concern digital RF transmitters, high-speed converters, mixed-signal design for RF and mmW communication systems, energy-efficient integrated systems, event-driven and neuro-inspired circuits for embedded machine learning. He was a co-recipient of a Best Student Paper Award at the 2011 Symposium on VLSI Circuits, a Best Paper Award at the 2020 IEEE AICAS Conference, and an Industrial Best Paper Award at the 2021 IEEE RFIC Symposium. He plays an active role as a board member of the France Section of the IEEE Circuits and Systems Society and Counselor of the IEEE Lille Student Branch.

Barry Cardiff (M '06) received the B.Eng., M.Eng. Sc., and Ph.D. degrees in electronic engineering from University College Dublin, Ireland, in 1992, 1995 and 2011, respectively. He was a Senior Design Engineer / Systems Architect for Nokia from 1993 to 2001, moving to Silicon & Software Systems (S3 group) thereafter as a Systems Architect in their R&D division focused on wireless communications and digitally assisted circuit design. Since 2013 he has been an Assistant Professor at University College Dublin, Ireland. His research interests are in digitally assisted circuit design and signal processing for wireless and optical communication systems. He holds several US patents related to wireless communication.

Deepu John (SM'14) received the B.Tech. degree in Electronics & Communication Engineering from the University of Kerala, India, in 2002, and the M.Sc. and Ph.D. degrees in electrical engineering from National University Singapore, Singapore, in 2008 and 2014, respectively. He is currently an Assistant Professor with the School of Electrical and Electronics Engineering, University College Dublin, Ireland. He was a Postdoctoral Researcher with the Bio-Electronics Lab, National University Singapore from 2014 to 2017. Previously, he worked as a Senior Engineer with Sanyo Semiconductors, Gifu, Japan. He is a recipient of the Institution of Engineers Singapore Prestigious Engineering Achievement Award in 2011, the Best Design Award at the Asian Solid-State Circuit Conference in 2013, and the IEEE Young Professionals, Region 10 Individual Award in 2013. He served as a member of the organizing committee/technical program committee for several IEEE conferences, including TENCON, ASICON, ISCAS, BioCAS, and ICTA. He served as a Guest Editor for IEEE Transactions on Circuits & Systems-I and IEEE Open Journal of Circuits & Systems. He serves as an Associate Editor for IEEE Transactions on Biomedical Circuits & Systems and Wiley International Journal of Circuit Theory & Applications. His research interests include low-power biomedical circuit design, energy-efficient signal processing, and edge computing.